Tropical nitric acid clouds

Mark Hervig[1] and Martin McHugh

G & A Technical Software, Newport News, Virginia, USA

[1] The presence of nitric acid clouds near the tropical tropopause was proposed over a decade ago, although little has been learned about them since. Particle extinction measurements at three wavelengths from the Halogen Occultation Experiment offer compelling evidence for the existence of nitric acid clouds near the tropical tropopause. Most of these clouds are consistent with nitric acid trihydrate, and a small fraction can be explained by liquid ternary H_2SO_4-H_2O-HNO_3 aerosols. *INDEX TERMS:* 0305 Atmospheric Composition and Structure: Aerosols and particles (0345, 4801); 0320 Atmospheric Composition and Structure: Cloud physics and chemistry; 3374 Meteorology and Atmospheric Dynamics: Tropical meteorology

1. Introduction

[2] Clouds composed of nitric acid condensates can form at temperatures below about 196 K. Globally, such temperatures occur only in the polar winter stratosphere and near the tropical tropopause. Polar stratospheric clouds (PSCs) have received considerable attention since the identification of their role in polar ozone loss. PSCs exist either as water ice, or nitric acid in the form of nitric acid trihydrate (NAT) or liquid ternary H_2SO_4-H_2O-HNO_3 aerosols (LTA). *Hamill and Fiocco* [1988] demonstrated the thermodynamic stability of nitric acid particles near the tropical tropopause. These clouds have received little attention, until the recent study by *Omar and Gardner* [2001] using space-borne lidar measurements. They suggested that over 30% of tropical near-tropopause clouds have optical characteristics similar to NAT, although further investigation was recommended to confirm the particle type.

[3] It is well known that upper tropospheric clouds (i.e., cirrus) impact the radiative balance of our climate system, and affect upper tropospheric and stratospheric water vapor budgets. Cirrus could also lead to ozone destruction through chlorine activation, although this suggestion was recently challenged [*Smith et al.*, 2001]. Like cirrus, nitric acid clouds could be important to climate and chemistry, but perhaps in ways that are not understood. For example, because nitric acid particles can completely sequester HNO_3 from the gas phase, particle sedimentation could remove or reposition HNO_3, thus affecting the odd nitrogen budget in the upper troposphere and stratosphere. NAT may also encourage ice nucleation and therefore play an important role in cirrus formation.

[4] This work identifies tropical nitric acid clouds (TNCs) in multi-wavelength particle extinction measurements from the Halogen Occultation Experiment (HALOE) (version 19). This work establishes a foothold for future studies of these largely unexplored phenomena.

2. HALOE Measurements

[5] HALOE has recorded solar occultation measurements from the Upper Atmosphere Research Satellite since October 1991. The limb transmissions measurements are used to infer profiles of aerosol extinction at four wavelengths (λ = 2.45, 3.40, 3.46, and 5.26 μm), seven gas mixing ratios (HF, HCl, CH_4, NO, NO_2, H_2O, and O_3), and temperature. The instrument field of view projected at the limb is 1.6 km vertically × 6 km horizontally. Optical effects and electronic smoothing yield an effective vertical resolution of ~2 km, corresponding to a tangent point path length of ~320 km. Aerosol extinctions are retrieved at the over-sampled vertical spacing of 0.3 km, and have uncertainties on the order of ±10–15% [*Hervig et al.*, 1996]. Below 35 km altitude, temperatures are taken from the National Center for Environmental Protection (NCEP) analysis.

[6] Cloud layers can have spatial dimensions that are smaller than or only partially intersect the HALOE sample volume. Because limb measurement retrievals assume spherical homogeneity, the altitude and magnitude of retrieved cloud extinctions could therefore be in error. Nevertheless, the identical volume of air is measured simultaneously by each HALOE channel. As a result, geometric sampling errors have an identical effect in each channel, so that relative spectral signatures deduced from HALOE are still accurate. In this work we primarily consider the ratios of extinctions at different wavelengths, which are insensitive to geometric sampling errors.

3. Physical Properties of TNCs

[7] The physical properties of TNCs were required to model HALOE cloud extinctions. Because little is known about TNC properties, their characteristics were estimated using nitric acid PSCs as a plausible analog. The most stable forms of nitric acid PSCs are NAT and LTA [*Koop et al.*, 1997] and both were considered for TNCs. TNC size distributions were estimated using in situ PSC measurements. Potential differences between TNCs and PSCs were estimated by determining properties of NAT and LTA under expected tropical tropopause conditions.

[8] The size distributions of nitric acid PSCs have been measured using balloon-borne optical particle counters (OPCs) over McMurdo Station, Antarctica [e.g., *Deshler et al.*, 1994]. These measurements yield lognormal size distributions with one or two modes, at height intervals of 0.5 km. To determine the properties of NAT particles, we examined 54 OPC profiles measured between 1989 and 1995. NAT was identified by comparing the measured temperatures and volumes (T_m and V_m) with calculated NAT temperatures and volumes (T_{NAT} and V_{NAT}) and ice frost points (T_{ice}). These calculations used HNO_3 and H_2O values which reflect late-winter conditions in the Antarctic stratosphere [*Hervig et al.*, 1997]. A measurement was classified as NAT when $T_{ice} < T_m < T_{NAT}$ and $2|V_m - V_{NAT}|/(V_m + V_{NAT}) < 1$ (575 distributions). These size distributions were typically bimodal with particle concentrations from 5 to 20 cm^{-3} and volume densities between 10^{-2} and 10 μm^3 cm^{-3} (Figure 1). LTA PSCs were similar to the NAT measurements in Figure 1.

[9] To further estimate TNC properties, relevant parameters near the tropical tropopause were explored. Radiosonde temperatures during 1990 – 2000 between 5°S and 5°N (~60,000 profiles) indicate that the most probable tropopause temperature and pressure were 190 K and 90 mbar. HALOE H_2O mixing ratios vary
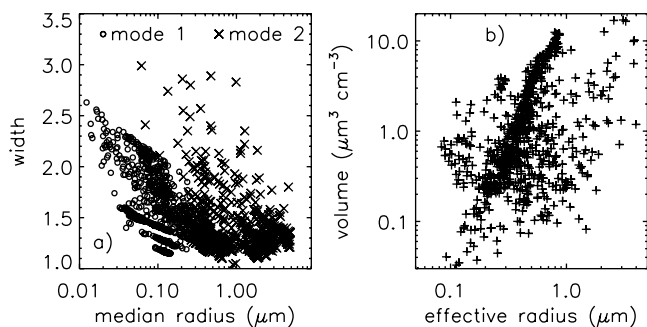
[1]Now at GATS Inc., Driggs, Idaho, USA.

Figure 1. (a) The width and median radius of lognormal size distributions measured in NAT PSCs. (b) Effective radius versus volume corresponding to the distributions in Figure 1a.

between about 2 and 6 ppmv near the equatorial tropopause. Differences between PSCs and TNCs are most likely due to the greater abundance of HNO_3 in the polar stratosphere (up to 15 ppbv) than near the tropical tropopause. HNO_3 measurements from the Microwave Limb Sounder (MLS) [e.g., *Lahoz et al.*, 1996] at 100 mbar pressure during 1993–1996 from 5°S–5°N (29,496 profiles) indicate a mode mixing ratio of 0.5 ppbv, and a mean value of 1.5 ± 1.4 ppbv. MLS retrieval errors can be large near the tropopause. In situ HNO_3 measurements near the tropical tropopause are lacking, however, the difference $NO_y - NO_x$ ($NO_x = NO + NO_2$) places an upper limit on HNO_3. In situ measurements of NO_y, NO, and NO_2 from the NASA ER-2 aircraft near the tropical tropopause on 12 occasions during 1994–1997 suggest between 0.1 and 0.4 ppbv HNO_3 [*Jensen and Drdla*, 2001]. The above data suggest that HNO_3 mixing ratios are probably less than 1 ppbv, but variable and perhaps near 3 ppbv.

[10] The above conditions were considered in calculations of equilibrium NAT and LTA volumes [e.g., *Carslaw et al.*, 1995]. LTA grow on background sulfate aerosols, and background aerosols were added to the NAT volumes. HALOE measurements after 1995 indicate 0.3 ppbv H_2SO_4, and this value was used in the volume calculations. Water vapor was set to initially 4 ppmv, and since near-tropopause H_2O is limited by ice growth, H_2O was kept at 90% of the ice saturation mixing ratio for $T < T_{ice}$. V_{NAT} and V_{LTA} versus temperature are shown in Figure 2a. V_{NAT} becomes asymptotic at low temperatures because NAT depletes the available HNO_3 and ceases to grow due to its fixed stoichiometry. LTA can grow at lower temperatures by water uptake after the available HNO_3 is depleted. The influence of HNO_3 on V_{NAT} and V_{LTA} is shown in Figure 2b. These results place reasonable limits on NAT and LTA volumes expected in TNCs. For $HNO_3 < 1.5$ ppbv, these results suggest $V_{NAT} < \sim1.3$ μm^3

cm^{-3} and $V_{LTA} < \sim1.8$ μm^3 cm^{-3}. In contrast, nitric acid PSCs have volumes greater than 10 μm^3 cm^{-3}, reflecting the greater abundance of HNO_3 in the polar stratosphere.

4. Identification of Cloud Type

[11] To identify cloud composition from HALOE extinction measurements, extinctions $\beta(\lambda)$ were calculated using Mie theory for clouds composed of ice, NAT, and LTA. These results revealed unique spectral signatures at the HALOE wavelengths.

[12] NAT and LTA extinctions were calculated using measured PSC size distributions (Figure 1). PSC volumes are greater than expected for TNCs, and the PSC size distributions were limited to volumes less than 1.3 μm^3 cm^{-3} for NAT and 1.8 μm^3 cm^{-3} for LTA. Considering larger volumes does not alter the conclusions below. NAT refractive indices at 196 K were taken from *Toon et al.* [1994], and LTA refractive indices were determined as a function of particle composition according to *Hervig et al.* [1997]. LTA compositions [*Carslaw et al.*, 1995] were determined for an OPC profile using measured temperatures and pressures with climatological H_2O and HNO_3. Because LTA grow on every background aerosol, a uniform composition was assumed for one size distribution measurement. NAT on the other hand, probably nucleate from a fraction of the background aerosols, and thus coexist with a large number of sulfate particles [*Koop et al.*, 1997]. This effect was treated in the NAT calculations by assigning NAT refractive indices to the large particle mode, and sulfate indices to the small particle mode. Because the dominant fraction of particle volume is in the large particle mode, using NAT refractive indices for all particle sizes produces only small changes in the results presented below. Ice (cirrus) extinctions were calculated using refractive indices from *Toon et al.* [1994] and lognormal size distributions with median radii from 0.1 to 10 μm and widths from 1.1 to 3 (effective radii, R_e, from 0.1–100 μm). Particle sizes included in these distributions encompass the range of cirrus particle sizes indicated by *Jensen et al.* [1994]. Below we use extinction ratios, which are independent of particle concentration. While our synthetic distributions are adequate, measured cirrus size distributions would be useful in future work. Background aerosols at the altitudes of interest are generally sulfate droplets [e.g., *Deshler et al.*, 1993]. Sulfate extinctions were calculated using sulfate refractive indices for 215 K [*Tisdale et al.*, 1998] and 60 wt.% H_2SO_4 (typical for the lower stratosphere), with sulfate size distributions from OPC measurements at middle latitudes

Figure 3. Extinction ratios calculated for sulfate aerosols and clouds composed of ice, NAT, and LTA. Ice results are bounded by the polygon for $\beta(2.45)/\beta(3.40) > 0.4$, and compact enough to be represented by a single curve for $\beta(2.45)/\beta(3.40) < 0.4$.
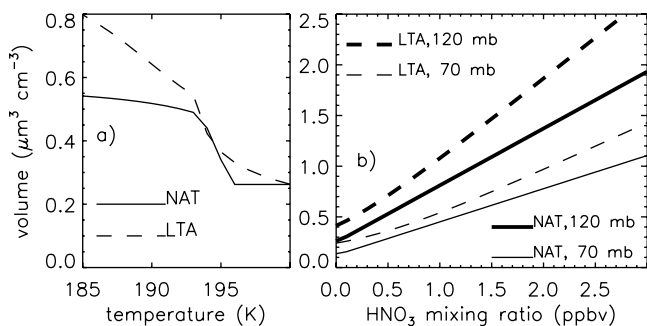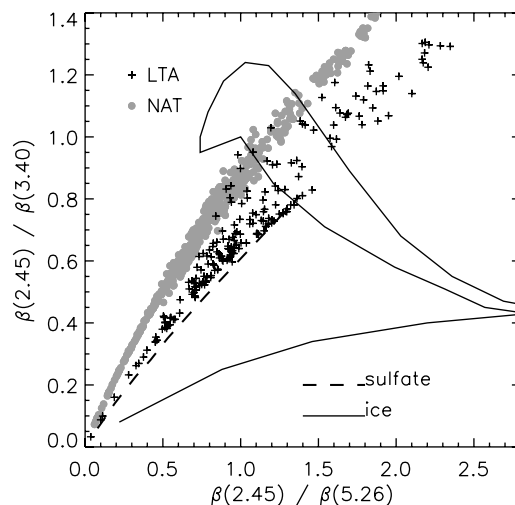

Figure 2. (a) NAT and LTA volume versus temperature calculated for 120 mbar pressure, 0.5 ppbv HNO_3, 0.3 ppbv H_2SO_4, and H_2O as described in text. (b) NAT and LTA volume versus HNO_3 calculated for two pressure levels, 188 K temperature, 0.3 ppbv H_2SO_4, and H_2O as described in text.
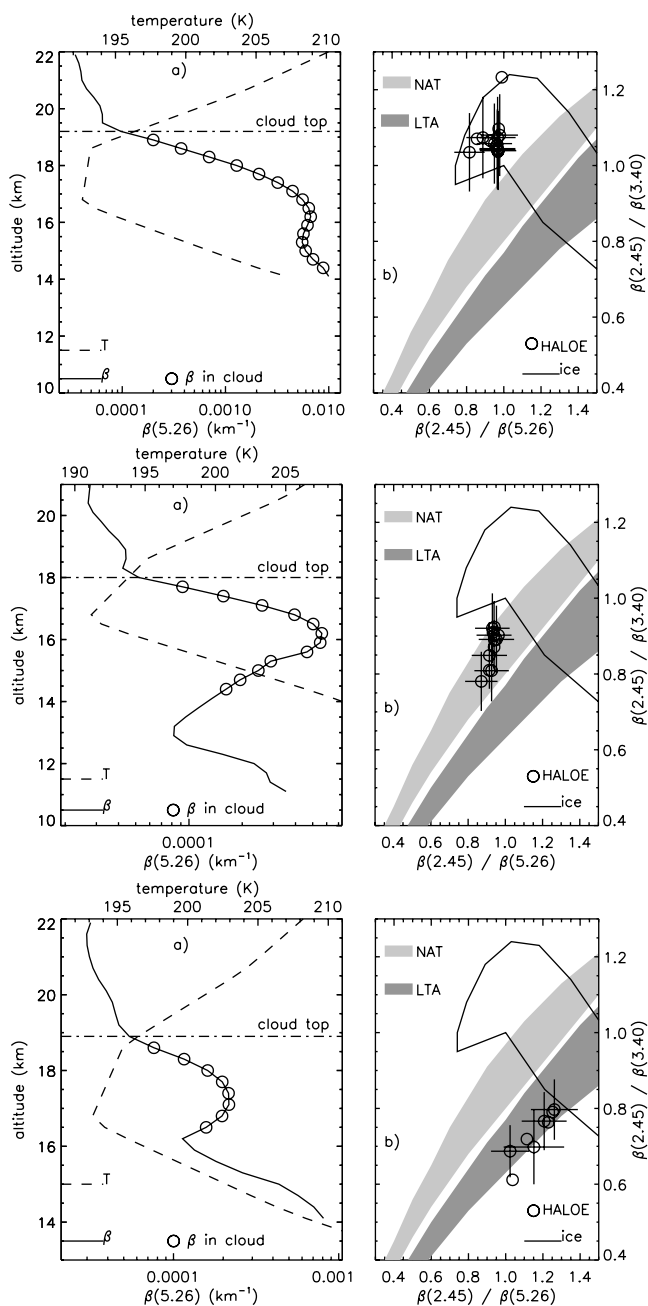
Figure 4. Examples of HALOE cloud measurements near the equator that were consistent with ice (top, October 1, 1997 at 3°N, 290°E), NAT (middle, December 25, 1998 at 0°N, 259°E), and LTA (bottom, March 1, 1997 at 3°N, 48°E). Symbols indicate HALOE measurements below cloud top where $0.8 < \beta(3.46)/\beta(3.40) < 1.2$. a) Profiles of HALOE extinction and NCEP temperature. Cloud top height is indicated. b) HALOE extinction ratios compared to model values for ice, NAT, and LTA. Error bars are shown on every other HALOE measurement.

[*Deshler et al.*, 1993]. Model extinction errors are difficult to quantify, but will stem from the refractive indices, size distributions, and optical theory.

[13] The modeled extinctions show spectral differences that are demonstrated using extinction ratios in Figure 3. NAT ratios are tightly clustered and separate from the LTA ratios, with the exception of a few points. Ice ratios occupy a broader range than NAT and LTA, and this is due primarily to the larger range of

ice particle sizes. Ice ratios with $\beta(2.45)/\beta(3.40) < 0.4$ correspond to $R_e < 1$ μm, and $\beta(2.45)/\beta(3.40) > 0.4$ correspond to R_e between 1 and 100 μm. In contrast, TNC effective radii were less than about 3 μm (Figure 1b). The sulfate ratios were compact enough to be represented by a single curve, which lies at the lower bound of the LTA results. In the region bounded roughly by $1 < \beta(2.45)/\beta(5.26) < 1.7$, NAT, LTA, and ice ratios all overlap, and HALOE measurements within this region cannot be classified. Despite some overlap, the modeled ratios lie in essentially distinct regions that can be used to classify cloud type in the HALOE measurements. For this purpose, modeled NAT and LTA ratios were described by curves bounding the model results.

5. Results Using HALOE Measurements

[14] Modeled extinction ratios for ice, NAT, and LTA were compared to HALOE cloud measurements near the tropical tropopause. Cloud tops were identified when the vertical extinction gradient, $G = [\log_{10}\beta(5.26)_i - \log_{10}\beta(5.26)_{i+1}] [Z_{i+1} - Z_i]^{-1}$, first exceeded 0.3 km^{-1} from the top down (Z_i = altitude at level i) [*Hervig and McHugh*, 1999]. Sulfate aerosols do not exhibit large positive gradients in the lower stratosphere, even under volcanic conditions. Measurements below cloud top were classified as NAT, LTA, or ice when the measured extinction ratios were consistent with model ratios for that particle type alone. To avoid false alarms from isolated measurement errors, we required that HALOE ratios be consistent with one model for at least four consecutive 0.3 km layers. Extinctions at 3.40 and 3.46 μm should be nearly equal for clouds and aerosols relevant to this work. The measured ratio $\beta(3.46)/\beta(3.40)$ therefore provides an assessment of measurement errors, and data were only used when $0.8 < \beta(3.46)/\beta(3.40) < 1.2$.

[15] Examples of ice, NAT, and LTA detected in equatorial HALOE measurements are shown in Figure 4. These results demonstrate that HALOE measurements can be consistent with model cloud predictions, to within the measurement uncertainty and over a broad vertical extent. HALOE measurements consistent with NAT and LTA offer compelling evidence for the existence of these cloud types near the tropical tropopause. NCEP temperatures (Figure 4) can have large uncertainties in the tropics, and these data were shown primarily to indicate thermal structure and tropopause height.

[16] Ice, NAT, and LTA occurrence frequencies were determined from HALOE as the ratio of clouds detected to the number of profiles examined. Zonal mean occurrence frequencies versus latitude are shown in Figure 5 for HALOE measurements during 1998. These results indicate that NAT and LTA are restricted to tropical latitudes, and that most TNCs are NAT (Figure 5a). NAT was most frequent near the equator, and zonal patterns in NAT occurrence reveal local maxima up to 40% (not shown). Ice also demonstrates an equatorial peak in occurrence rate, and roughly 8 in 10 equatorial clouds are ice (Figure 5b). Zonal minimum tropopause temperatures (T_{min}) from NCEP analysis were compared to T_{NAT} calculated for average tropopause conditions and 0.5 ppbv HNO_3 (Figure 5a). T_{min} decreases sharply within the tropics, and is below T_{NAT} over the same latitude range where HALOE indicates the presence of NAT. While not a strict validation, the agreement between HALOE and temperature patterns lends confidence to the HALOE NAT measurements.

[17] Radiosonde temperatures measured during 1990–2000 between 5°S and 5°N were examined (~60,000 profiles). T_{NAT} was computed for each sounding using constant HNO_3 and monthly mean H_2O profiles from equatorial HALOE measurements. These data revealed that temperatures near the tropical tropopause were below T_{NAT} in ~80% (95%) of the soundings, assuming 0.3 (1.0) ppbv HNO_3. This result is in sharp contrast
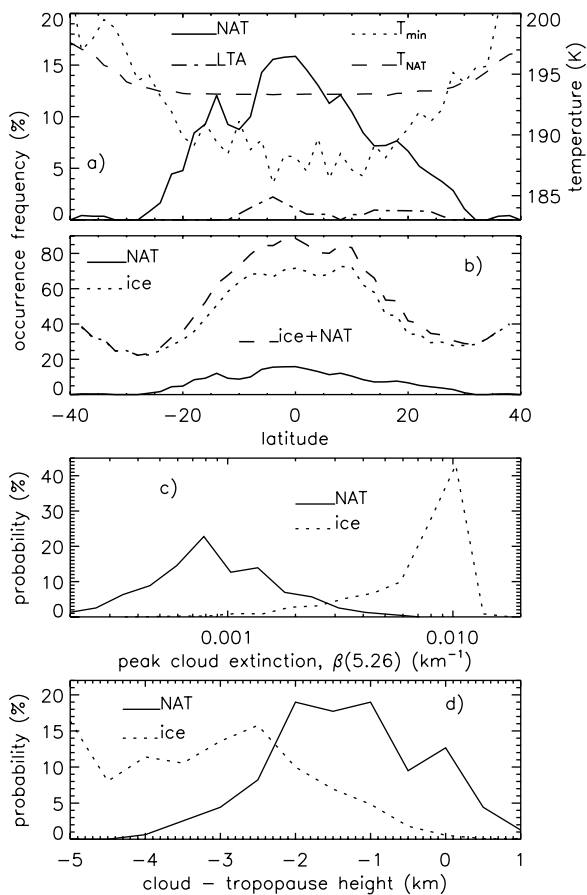
Figure 5. Cloud properties derived from HALOE measurements during 1998 at latitudes from 40°S to 40°N. (a) Zonal mean NAT and LTA occurrence frequency versus latitude. Also shown are zonal minimum tropopause temperatures (T_{min}) from NCEP analysis during 1998, and T_{NAT} calculated for 0.5 ppbv HNO_3. Zonal mean NCEP tropopause temperatures are roughly 5 K higher than T_{min}. T_{ice} at the tropopause is about 4 K lower than T_{NAT}. (b) Zonal mean occurrence frequencies of ice, NAT, and the sum of ice and NAT. (c) Probability distributions of peak cloud extinction. Peak extinctions were taken as the maximum extinction in each cloud identified. (d) Probability distributions of the altitude where the peak extinction occurred relative to tropopause height.

to the relatively low NAT occurrence rates determined from HALOE. This discrepancy may reflect a barrier to NAT nucleation. A similar quandary exists in the polar winter stratosphere, where NAT is not always observed at temperatures below T_{NAT}.

[18] Probability distributions of peak cloud extinction, and peak cloud extinction altitude relative to the tropopause are shown in Figures 5c and 5d. The brightest NAT layers were 1 – 2 km below the tropopause, and ice layers were generally below NAT. While peak NAT extinctions may have been expected at the tropopause, lower altitudes are consistent with particle sedimentation and accumulation [Eric Jensen, personal communication]. Ice extinctions were narrowly distributed about 10^{-2} km^{-1}, which is near the limit for complete opacity in the limb view. NAT extinction can be related to volume, $V_{NAT} = 1488\ \beta(5.26)^{0.984}$ [*Hervig et al.,* 1997], and HALOE suggests V_{NAT} from roughly 0.6 to 2 μm^3 cm^{-3}. $V_{NAT} < \sim 1$ μm^3 cm^{-3} is generally consistent with $HNO_3 < \sim 1$ ppbv (Figure 2b). Larger NAT volumes suggest more HNO_3 than is generally thought to exist near the tropical tropopause, although

MLS does suggest HNO_3 mixing ratios over 1 ppbv. In any case, further investigation is required in this area.

6. Summary

[19] Multi-wavelength particle extinction measurements from HALOE show the existence of NAT and LTA clouds near the tropical tropopause. This finding was based on spectral identification using model predictions of the HALOE response to ice, NAT, and LTA. HALOE observations indicate that NAT is the dominant particle type in TNCs, and show a latitudinal NAT distribution that is consistent with temperature patterns. Two conundrums arise from this work. First, the tropical tropopause is saturated with respect to NAT nearly all the time, yet HALOE indicates NAT occurrence frequencies of about 15%. Second, NAT volumes inferred from HALOE often imply more HNO_3 near the tropical tropopause than is generally expected. Future work will address these questions, and further explore TNCs using 10+ years of HALOE measurements.

References

Carslaw, K. S., B. P. Luo, and T. Peter, An analytic expression for the composition of aqueous HNO_3-H_2SO_4 stratospheric aerosols including gas phase removal of HNO_3, *Geophys. Res. Lett.*, *22*, 1877–1880, 1995.

Deshler, T., B. J. Johnson, and W. R. Rozier, Balloonborne measurements of Pinatubo aerosol during 1991 and 1992 at 41°N, vertical profiles, size distribution, and volatility, *Geophys. Res. Lett.*, *20*, 1435–1438, 1993.

Deshler, T., B. J. Johnson, and W. R. Rozier, Changes in the character of polar stratospheric clouds over Antarctica in 1992 due to the Pinatubo volcanic aerosol, *Geophys. Res. Lett.*, *21*, 273–276, 1994.

Hamill, P., and G. Fiocco, Nitric acid aerosols at the tropical tropopause, *Geophys. Res. Lett.*, *15*, 1189–1192, 1988.

Hervig, M. E., J. M. Russell III, L. L. Gordley, J. Daniels, J. H. Park, S. R. Drayson, and T. Deshler, Validation of aerosol measurements from the Halogen Occultation Experiment, *J. Geophys. Res.*, *101*, 10,267–10,275, 1996.

Hervig, M. E., K. S. Carslaw, Th. Peter, T. Deshler, L. L. Gordley, G. Redaelli, U. Biermann, and J. M. Russell III, Polar stratospheric clouds due to vapor intrusions: HALOE observations of the Antarctic vortex in 1993, *J. Geophys. Res.*, *102*, 28,185–28,193, 1997.

Hervig, M. E., and M. McHugh, Cirrus detection using HALOE measurements, *Geophys. Res. Lett.*, *26*, 719–722, 1999.

Jensen, E., and K. Drdla, Nitric acid concentrations near the tropical tropopause: Implications for the properties of tropical nitric acid trihydrate clouds, *Geophys. Res. Lett.*, submitted, 2001.

Jensen, E. J., O. B. Toon, D. L. Westphal, S. Kinne, and A. J. Heymsfield, Microphysical modeling of cirrus 1. Comparison with 1986 FIRE IFO measurements, *J. Geophys. Res.*, *99*, 10,421–10,442, 1994.

Koop, T., K. S. Carslaw, and Th. Peter, Thermodynamic stability and phase transitions of polar stratospheric cloud particles, *Geophys. Res. Lett.*, *24*, 2199–2202, 1997.

Lahoz, W. A., et al., Validation of UARS Microwave Limb Sounder 183 GHz H_2O measurements, *J. Geophys. Res.*, *101*, 10,129–10,149, 1996.

Omar, A. H., and C. S. Gardner, Observations by the Lidar In-Space Technology Experiment (LITE) of high-altitude cirrus clouds over the equator in regions exhibiting extremely cold temperatures, *J. Geophys. Res.*, *106*, 1227–1236, 2001.

Smith, J. B., E. J. Hinsta, N. T. Allen, R. M. Stimpfle, and J. G. Anderson, Mechanisms for midlatitude ozone loss: Heterogeneous chemistry in the lowermost stratosphere?, *J. Geophys. Res.*, *106*, 1297–1309, 2001.

Tisdale, R. T., D. L. Glandorf, M. A. Tolbert, and O. B. Toon, Infrared optical constants of low-temperature H_2SO_4 solutions representative of stratospheric sulfate aerosols, *J. Geophys. Res.*, *130*, 25,353–25,370, 1998.

Toon, O. B., M. A. Tolbert, B. G. Koehler, A. M. Middlebrook, and J. Jordan, Infrared optical constants of H_2O ice, amorphous nitric acid solutions, and nitric acid hydrates, *J. Geophys. Res.*, *99*, 25,631–25,645, 1994.

M. Hervig, GATS, Inc., 65 South Main St. Suite 5, P.O. Box 449, Driggs, Id 83422, USA.

M. McHugh, G & A Technical Software, Newport News, VA, USA.